# Mechanistic Insights into Metal Lewis Acid-Mediated Catalytic Transfer Hydrogenation of Furfural to 2-Methylfuran

Matthew J. Gilkey, Paraskevi Panagiotopoulou, Alexander V. Mironenko, Glen R. Jenness, Dionisios G. Vlachos,* and Bingjun Xu*

Catalysis Center for Energy Innovation, Department of Chemical and Biomolecular Engineering, University of Delaware, Newark, Delaware 19716, United States

Ⓢ *Supporting Information*
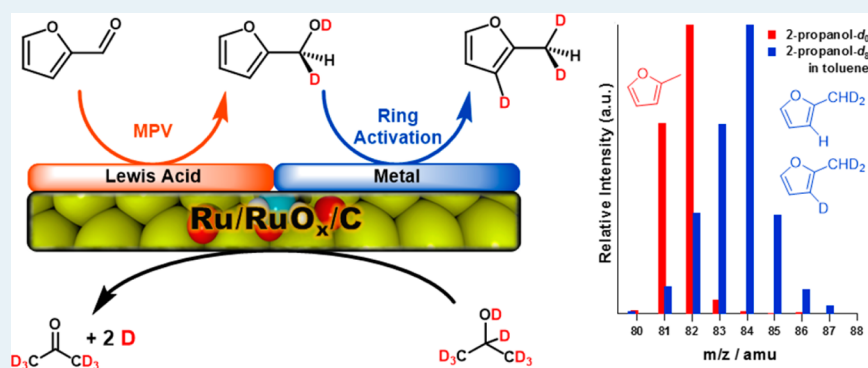
ABSTRACT: Biomass conversion to fuels and chemicals provides sustainability, but the highly oxygenated nature of a large fraction of biomass-derived molecules requires removal of the excess oxygen and partial hydrogenation in the upgrade, typically met by hydrodeoxygenation processes. Catalytic transfer hydrogenation is a general approach in accomplishing this with renewable organic hydrogen donors, but mechanistic understanding is currently lacking. Here, we elucidate the molecular level reaction pathway of converting hemicellulose-derived furfural to 2-methylfuran on a bifunctional Ru/RuO$_x$/C catalyst using isopropyl alcohol as the hydrogen donor via a combination of isotopic labeling and kinetic studies. Hydrogenation of the carbonyl group of furfural to furfuryl alcohol proceeds through a Lewis acid-mediated intermolecular hydride transfer and hydrogenolysis of furfuryl alcohol occurs mainly via ring-activation involving both metal and Lewis acid sites. Our results show that the bifunctional nature of the catalyst is critical in the efficient hydrodeoxygenation of furanics and provides insights toward the rational design of such catalysts.

KEYWORDS: catalytic transfer hydrogenation, bifunctional, mechanism, ring activation, furfural

■ INTRODUCTION

The multifunctional nature of biomass-derived feedstocks demands intricate interaction between the reactant molecule and the catalyst surfaces to remove the excess oxygen and partially hydrogenated specific unsaturated groups for many relevant chemicals and fuels, a process known as hydrodeoxygenation (HDO). In doing so, one needs to avoid overhydrogenation and unselectively cracking the C−C bonds of the molecule. This tandem of reactions typically employs a Brønsted acid catalyst, such as sulfuric acid, to remove oxygen as water, and a metal catalyst, such as Pt, to carry out the hydrogenation using high-pressure hydrogen.[1−4] Such dual metal/Brønsted acid catalysts can be environmentally harsh, and strong Brønsted acid catalysts can lead to side reactions and reduce selectivity. Development of more selective processes and catalysts can have a profound impact on the viability of biomass upgrade.[1,5,6]

A selective route to remove excess oxygen-containing functional groups in biomass-derived feedstocks is via catalytic transfer hydrogenation (CTH), which employs renewable organic compounds such as alcohols and organic acids as the hydrogen donor. Because biomass is typically availabe in remote areas that lack a transportation system, CTH is an attractive alternative to alleviate the need for high-pressure hydrogen that requires large-scale infrastructure, available only in integrated chemical plants.[7−9] CTH has been demonstrated in the upgrade of various biomass molecules, including cellulose, sugars, and furanics, often employing a supported metal or metal oxides as a hydrogenation catalyst.[10−13] In doing so, a variety of hydrogen sources have been successfully used, including linear alcohols (2-propanol, methanol, etc.),[10] cyclohexanol,[13] and formic acid.[9,12] Pathways such as hydrogenation of levulinic acid to γ-valerolactone using metal oxide catalysts,[10] as well as ring opening from 5-

hydroxymethylfurfural (HMF) using formic acid over a Pd catalyst[9] have been studied with success. Currently, the mechanism of CTH remains elusive, which prevents the development of less costly and more efficient catalysts.

Our previous studies established that CTH with an alcohol as the hydrogen donor is an effective pathway to convert furfural to 2-methylfuran (MF) over a mildly oxidized Ru/C catalyst with high yield (76%).[14,15] Neither Ru/C nor RuO_2 shows MF yield nearly as high as the partially oxidized Ru/C ($Ru/RuO_x/$C), suggesting that multiple sites are at play on $Ru/RuO_x/$C. The oxidation of Ru/C creates a bifunctional catalyst,[16−18] consisting of coexisting metal (Ru) and Lewis acid (RuO_x) sites, and this bifunctionality is key to achieving high performance without hydrogenating the furan ring or cracking the C−C bonds. Unlike with metal/Brønsted acid catalysts, fewer side reactions can occur; however, neither the role of each functionality nor their cooperativity is clear.

Herein, we present a mechanistic study on the reaction pathways in the CTH of furfural over a mildly oxidized Ru/C catalyst, referred to as $Ru/RuO_x/$C, by detailed mass fragmentation analysis with isotopically labeled chemicals and rigorous kinetic studies. Furfural is an ideal biomass-derived "platform" chemical, and its hydrogenolysis product, MF, has a high octane number and can be employed for the production of renewable toluene.[19−21] We show that the intermolecular hydride transfer is the dominant pathway for the hydrogenation of the carbonyl group of furfural to furfuryl alcohol (FA). Further, hydrogenolysis via ring activation is a major, if not the dominant, pathway in the C−OH bond cleavage in the conversion of FA to MF. Our results provide molecular level understanding of the role of the cooperativity of metal and Lewis acid sites in mediating the CTH of biomass derivatives, which can guide the rational design of efficient bifunctional catalysts by suitable choice and proper atomic level arrangement of Lewis acid and metal sites. Further, we demonstrate that detailed mass fragmentation analysis is a powerful technique in mechanistic investigations of complex reactions involving biomass-derived molecules.

METHODS

Materials and Catalyst Preparation. All chemicals were obtained from Sigma-Aldrich and used without further purification. The catalyst used was 5 wt % Ru/C (Sigma-Aldrich), which, prior to each experiment, was treated for 3 h at 300 °C in H_2 flow of 40 cc/min, followed by mild oxidation for 3 h at 130 °C in 5% O_2/He flow (40 cc/min).

Catalyst Evaluation. Catalytic transfer hydrogenation of furfural was carried out in a 100 mL Parr batch reactor. In a typical experiment, the reactor was charged with 24 mL of a 10 vol % 2-propanol (unlabeled (-d_0) or perdeuterated(-d_8))/toluene solution of furfural (1 wt %) and 0.1 g of $Ru/RuO_x/$C catalyst, pressurized to 300 psi (2.04 MPa) with N_2 and heated to a predetermined temperature. It typically takes ∼30 min for the reactants to reach the desired temperature, which is not included in the reported reaction time. Reaction was quenched by soaking the reactor in an ice bath upon reaching the desired reaction time. The suspension in the reactor was collected after it reached room temperature, filtered, stored in sealed vials, and analyzed.

Analytical Methods. Identification of the liquid phase products was performed on a gas chromatography−mass spectrometry (GC/MS, Shimadzu QP2010 Plus) system. The GC (Shimadzu GC2010) is equipped with an HP-INNOWax

capillary column (30 m × 0.25 mm id ×0.50 μm film thickness) and interfaced directly to the MS (Shimadzu QP2010 Plus). Identification of the GC/MS spectral features was accomplished by comparing the mass fragmentation pattern of the products with those in the built-in Wiley/NIST library. The shift in the mass spectrum of each product obtained using perdeuterated 2-propanol (2-propanol-d_8) as the hydrogen donor was reported relative to that obtained using unlabeled 2-propanol (2-propanol-d_0), primarily focusing on the shifts of the parent ion of the molecules.

Quantification of the liquid products was achieved using a gas chromatograph (GC, Agilent 7890A), equipped with an HP-INNOWax capillary column (30 m × 0.25 mm id ×0.5 μm film thickness) and an FID detector. Response factors were determined using self-prepared solutions of known concentration. The kinetic isotope effect (KIE) was calculated from the ratio of the reaction rate constants obtained from kinetic data, using both furfural and FA as starting reagents. Rate constants were estimated by analyzing the experimental data with a proposed reaction network using a nonlinear least-squares method (a more detailed description is available in the main text and Supporting Information).

Computational Methods for Adsorption Energy Calculations. Density functional calculations were performed using VASP software.[22−25] Core electrons were represented using PAW formalism,[26,27] and valence electrons were modeled with the exchange-correlation functional of Perdew, Burke, and Ernzerhof (PBE).[28] Ground state energies were calculated self-consistently using a plane wave basis set with a kinetic energy cutoff of 400 eV, an electronic energy threshold of 10^{-6} eV, and a force tolerance of 0.05 eV/Å. Lattice constants were determined in a bulk calculation, employing 3 × 3 × 3 and 15 × 15 × 15 Monkhorst−Pack[29] k-point mesh for RuO_2 and Ru, respectively. The values were found to be a = 4.54 and c = 3.08 Å for the RuO_2 rutile structure and a = 2.70 and c = 4.26 Å for the hcp Ru lattice. The (110) crystal plane of RuO_2 was modeled in a p(3 × 2) supercell with one relaxed and three unrelaxed layers of O−Ru−O units; the reciprocal space was sampled at the Γ-point. The p(3 × 3) repetition was employed for the Ru(0001) surface. Among four layers of atoms, two bottom layers remained fixed in their bulk coordinates. The reciprocal space was sampled using the (3 × 3 × 1) Monkhorst−Pack k-point grid. Adsorption energies were calculated in a conventional way as

$$\Delta E_{ads} = E_{ads+slab} - E_{ads} - E_{slab}$$

Here, ΔE_{ads}, $E_{ads+slab}$, E_{ads}, and E_{slab} are adsorption energy, energy of a species adsorbed on a slab, energy of a species in vacuum, and energy of the slab, respectively.

RESULTS AND DISCUSSION

The hydrodeoxygenation (HDO) of furfural to MF (Scheme 1) entails, first, the hydrogenation of the carbonyl group of furfural to form FA. The chemistry can proceed via classic metal-mediated hydrogenation, that is, the atomic hydrogen adsorbed on metal sites, formed from the dehydrogenation of alcohols, adds to the C and O in the carbonyl group. We hypothesize that an alternative pathway is the Lewis acid-mediated intermolecular hydride transfer of the β-H in the alcohol to the carbonyl group, following the Meerwein−Ponndorf−Verley (MPV) mechanism.[7,30−33] Because of coexistence of metal (Ru) and Lewis acid (RuO_x) sites, both pathways could be at play simultaneously. Upon production of FA, hydrogenolysis

Scheme 1. Potential Reaction Pathways in the HDO of Furfural to MF
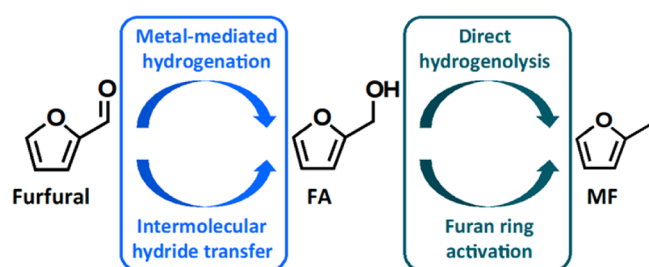
could proceed either via the direct route (i.e., the cleavage of the C−OH bond followed by H addition) or via the activation of the furan ring, in which H is added to the ring to break the ring aromaticity and facilitate OH removal. Currently, the pathway through which the metal and Lewis acid sites contribute to the reactivity is unclear.

■ **ISOTOPIC LABELING STUDIES OF CATALYTIC TRANSFER HYDROGENATION OF FURFURAL TO MF**

Hydrogenation of Furfural to FA. The mass fragmentation pattern of FA produced with 2-propanol-d_0 as the hydrogen donor at 140 °C in toluene matches well that in the NIST database.[34] The parent ion of FA (98 amu) is the

most intense peak (red bars in Figure 1a), and the small signal in 99 amu is attributed to the natural isotope abundance of [13]C. A clear mass shift by 1 amu was observed when 2-propanol-d_8 was used as the hydrogen donor under otherwise identical reaction conditions (blue bars in Figure 1a), indicating that the produced FA molecule contains one D. In both hydrogenation mechanisms (Scheme S1), the FA molecule contains two Ds using 2-propanol-d_8. The discrepancy between the predicted and observed mass shifts (2 and 1 amu, respectively) can be rationalized by the fact that the deuterium in the OD group of FA can exchange the OH groups in the capillary gas chromatograph (GC) column, as evidenced by the injection of neat 2-propanol-d_8 (Figure S2). Therefore, we conclude the 1 amu mass shift in the FA formed with 2-propanol-d_8 as the hydrogen donor originates from the D bonded to the hydroxymethyl carbon (Figure 1d).

Since FA formed via either mechanism has an identical isotopic structure, replacing 2-propanol-d_0 with 2-propanol-d_8 cannot differentiate the two mechanisms. The key difference between the two reaction pathways (Figure 1d and e) is whether the H being transferred adsorbs onto the catalyst surface. The MVP mechanism proceeds via the formation of a six-membered ring configuration, through which the β-H of 2-propanol is transferred to the carbonyl C atom of furfural. The H transfer occurs in a concerted step, in which the H being transferred never adsorbs onto the surface of the catalyst. Therefore, when 2-propanol-d_8 is used as the hydrogen donor,
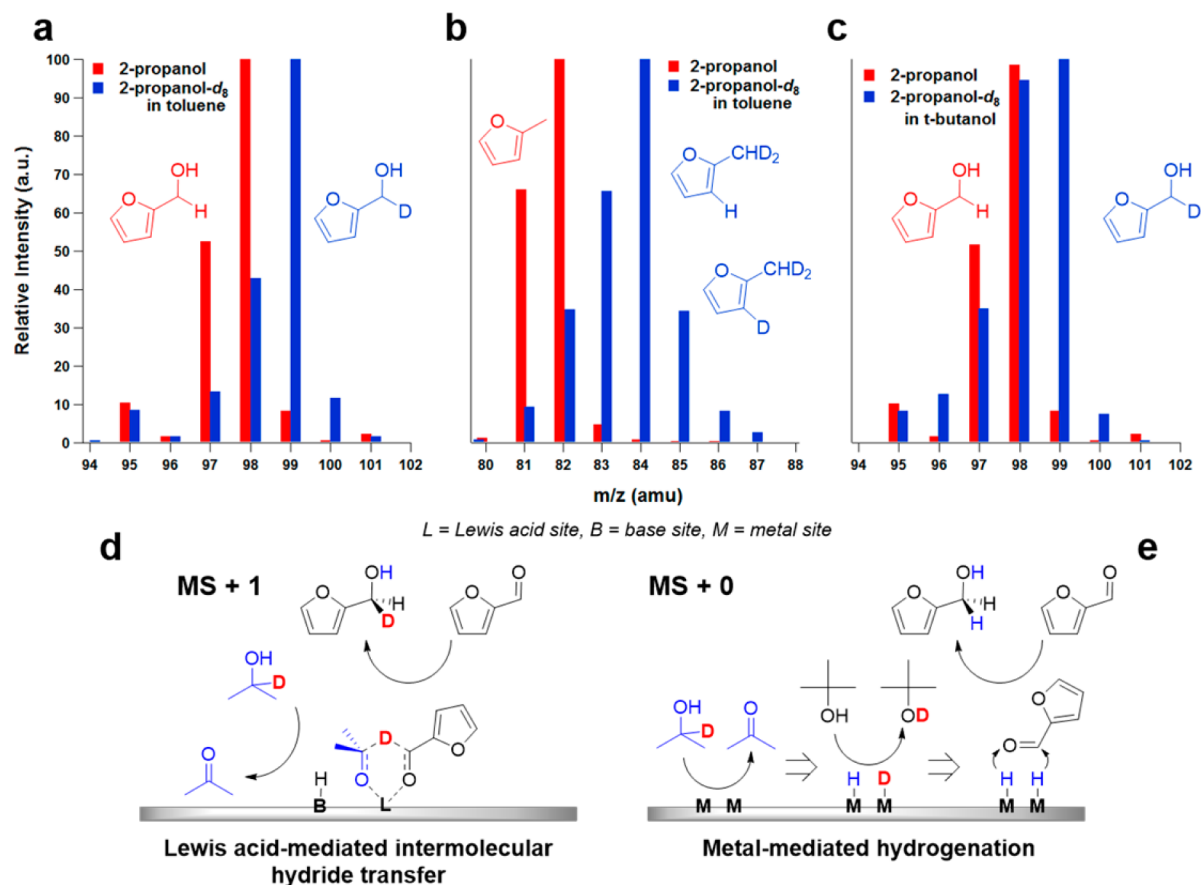

Figure 1. Mass fragmentation analysis of the products of CTH of furfural. Mass spectra (all intensities scaled to 100%) of (a) FA, (b) MF obtained after furfural hydrogenolysis in toluene, and (c) FA obtained from furfural hydrogenolysis in *t*-butyl alcohol. Schematic of the reaction mechanism of FA formation via (d) Lewis acid-mediated intermolecular hydride transfer and (e) metal-mediated hydrogenation. Experimental conditions: 1 wt % furfural in 10% 2-propanol-d_0 or -d_8 in toluene solution; C_{cat} = 4.1 g L^{-1}; 2.04 MPa N$_2$, T = 140 °C, and reaction time 8.5 h.
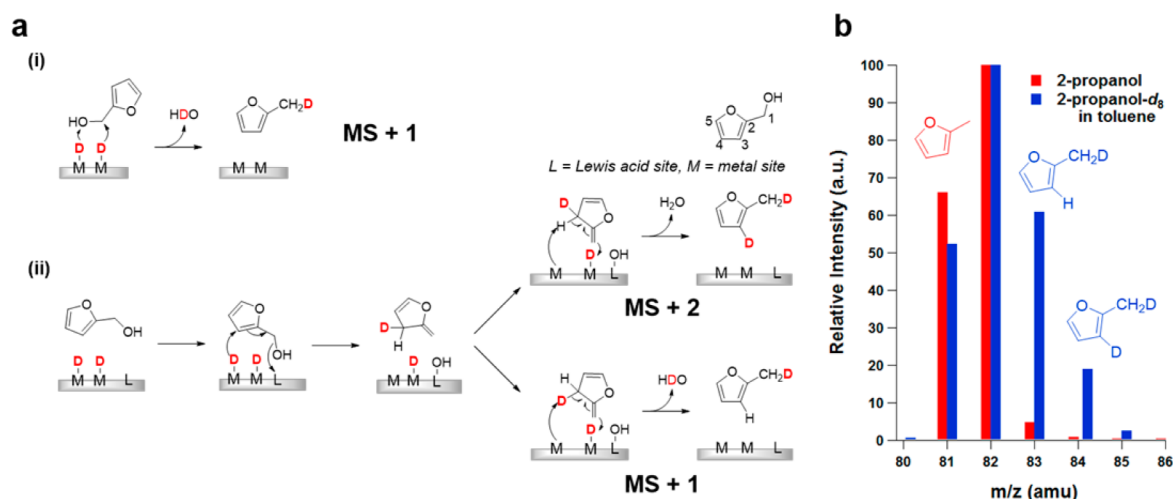
Figure 2. Reaction mechanism for the hydrogenolysis of FA to MF. (a) Schematic of two potential pathways: (i) direct hydrogenolysis and (ii) hydrogenolysis via furan ring activation. (b) Mass spectrum of MF obtained after FA hydrogenolysis. Experimental conditions: 1 wt % FA in 10% 2-propanol-d_0 or d_8 in toluene solution, C_{cat} = 4.1 g L^{-1}, 2.04 MPa N$_2$, T = 140 °C, and reaction time 5 h.

the β-D will be directly transferred to the carbonyl C atom in furfural. In contrast, two consecutive reaction steps are involved in the metal-mediated hydrogenation: first, dehydrogenation of 2-propanol occurs on metallic sites to form adsorbed H atoms and acetone, followed by the addition of the adsorbed hydrogen atoms to the carbonyl bond. In this pathway, *all hydrogen atoms transferred are adsorbed onto the metallic sites prior to being added to the carbonyl group of furfural.*

To differentiate these two possible pathways, we replaced toluene with *t*-butyl alcohol as solvent in the reaction because (1) as a tertiary alcohol, the absence of β-H prevents it from acting as a hydrogen donor; and (2) the H in the OH group of *t*-butyl alcohol is able to exchange with active H atoms on the catalyst (e.g., O−H and Ru−H) while leaving the H in the C−H bonds untouched. Because *t*-butyl alcohol is in great excess (~90 mol %) with respect to 2-propanol, most of the OD in 2-propanol-d_8 will be exchanged into OH because of the fast OH/OD exchange between alcohols. Thus, 2-propanol-d_7 (CD$_3$CD(OH)CD$_3$) is the majority of the D (or H) donor when 2-propanol-d_8 is used. In the case of an MVP pathway, the only D transferred to furfural is the β-D of 2-propanol-d_7 because it is unexchanged and is transferred via a concerted pathway without adsorbing on a metallic site (Figure 1d). Thus, a 1 amu MS shift of the FA formed is expected. In contrast, FA formed following the metal-mediated hydrogenation is expected to be free of D (no mass shift), because the fast H/D exchange between *t*-butyl alcohol and adsorbed D will replace most of the adsorbed D with H (Figure 1e).

FA formed in the hydrogenation of furfural with 2-propanol-d_0 and -d_8 in *t*-butyl alcohol clearly shows a mass shift of the parent ion by 1 amu (from 98 to 99 amu, Figure 1c), indicating that the concerted intermolecular hydride transfer mechanism (MPV) is the dominant pathway in the hydrogenation of the carbonyl group of furfural. There are two major assumptions in this analysis: (1) the H/D exchange between the OH and OD groups in alcohols occurs very rapidly,[35,36] which is well established, and (2) the H/D exchange between OH of *t*-butyl alcohol and adsorbed D is also facile, the evidence of which is provided in the Supporting Information (Figure S2).

Although dehydrogenation of the alcohols under our reaction conditions is rather facile, the strong adsorption of furanics on the oxophilic Ru sites suppresses the metal-mediated

mechanism (see below). In contrast, the concerted Lewis-acid-catalyzed mechanism is not retarded by site blocking and induces the hydrogenation of the carbonyl group.

Hydrogenolysis of FA to MF. The cleavage of the C−OH bond in FA via hydrogenolysis to MF can proceed via either a direct route or the activation of the aromatic ring (Figure 2a). In the former, the C−OH bond cleavage is followed by the addition of an adsorbed H atom on metallic sites. The direct hydrogenolysis pathway with 2-propanol-d_8 will lead to the formation of MF containing 1 D atom bonded to C$_1$, with a mass shift of the parent ion of MF by 1 amu.

In ring activation, a surface-adsorbed D, formed via the dehydrogenation of 2-propanol-d_8 on Ru sites, adds to C$_3$ (instead of the C$_5$; see below) and causes the furan ring to lose its aromaticity by shifting the double bond between C$_2$ and C$_3$ to C$_1$ and C$_2$, which in turn drives the cleavage of the C−OH bond, forming an unstable reaction intermediate (Figure 2a(ii)). We hypothesize that the OH is bonded to a Lewis acid site after the scission of the C−OH bond as a result of the high coverage of oxygenates, that is, furfural and FA, on the Ru sites. This step is followed by H abstraction from C$_3$, which reforms the double bond between C$_2$ and C$_3$ while C$_1$ gets a D from the surface. The MF formed is expected to contain 2 Ds and exhibit a mass shift of the parent ion by 2 amu. Importantly, the H and D bonded to C$_3$ are equivalent, and thus, another equally likely pathway is for the catalyst to abstract the D from C$_3$ and the C$_1$ to obtain a D from the surface. MF formed from this route contains only 1 D and, thus, exhibits a mass shift of the parent ion by 1 amu. Thus, the proposed ring activation mechanism predicts a mixture of mass shifts of the parent ion of MF of 1 and 2 amu (Figure 2a).

MF formed from the reaction between FA and 2-propanol-d_8 clearly shows the shifts of the parent ion by up to 2 amu (Figure 2b), consistent with the proposed hydrogenolysis mechanism involving ring activation. The red and blue bars correspond to the mass fragments of MF formed via the reaction of FA with 2-propanol-d_0 and 2-propanol-d_8, respectively. The signals at 83 and 84 amu, corresponding to mass shifts of the parent ion of MF by 1 and 2 amu, respectively, are significantly higher for red bars, indicating that up to 2 Ds in 2-propanol-d_8 end up in MF. We conclude that C−OH cleavage via aromatic ring activation is a major pathway

in the hydrogenolysis of FA. On the basis of the intensity of 83 and 84 amu signals, roughly half of MF is estimated to form via the ring activation pathway. In addition, MF formed via the reaction of furfural and 2-propanol-d_8 exhibits mass shifts of the parent ion by up to 3 amu (Figure 1b), consistent with the fact that the hydrogenation of the carbonyl group introduces 1 D and the hydrogenolysis of FA introduces 1 or 2 Ds.

H/D exchange on C_5 (unprotected α-carbon) of MF in the presence of 2-propanol-d_8 also introduces D to MF. However, the majority of deuterium incorporated in MF originates from the ring activation pathway described above. This can be shown by observing similar +2 and +3 mass shifts in 2,5-dimethylfuran formed with 5-methylfurfural as the reactant, in which there is no unprotected α-carbon (Scheme S3 and Figure S3). Additional evidence of ring activation is demonstrated by the reaction of furfural-d_3 with 2-propanol-d_0, in which furfural-d_3 contains deuterium bonded to the 3 carbon atoms in the ring (Scheme S4 and Figure S4).

■ KINETIC MEASUREMENTS

Pronounced kinetic isotope effects in the HDO of furfural and FA with 2-propanol-d_0/d_8 are consistent with the proposed mechanism based on the isotopic labeling experiments. Aside from the hydrogenation of furfural and hydrogenolysis of FA discussed above, reversible etherification between FA and 2-propanol was also observed. Kinetic data (Figure 3) reveal that both hydrogenation and hydrogenolysis steps exhibit a significant KIE (Table 1; eqs S6−S9 for the kinetic model), thereby indicating that the breaking of a C−H bond is rate-limiting in both steps. The KIE of the hydrogenation of furfural (k_1) of 1.7 is consistent with the MPV reaction in which the breaking of the C−H bond at the β-carbon in 2-propanol is rate-limiting. A KIE of 1.3 for FA hydrogenolysis (when starting from furfural) suggests that the rate of reaction is limited by the breaking of a C−H bond. This is an interesting result because hydrogenolysis of FA to MF is supposed to break the C−OH bond; however, the C−H bond breaking can occur in the dehydrogenation of 2-propanol or ring activation step. In contrast, etherification does not involve the breaking of a C−H bond, and no KIE is expected, as confirmed herein. A KIE of 1.6 in k_2 when starting from FA (Figure 3c) confirms that the breaking of the C−H bond, rather than the C−O bond scission, is rate-limiting in the hydrogenolysis step, in good agreement with the KIE observed when starting from furfural. In addition, no KIE is observed for the etherification pathway when starting from FA.

■ IMPLICATIONS OF MECHANISTIC FINDINGS ON CATALYST DESIGN

Our mechanistic studies illustrate the importance of bifunctional metal and Lewis acid catalysis in furfural hydrodeoxygenation. In particular, hydrogenation of the carbonyl group of furfural to FA proceeds primarily via an intermolecular hydride transfer mechanism enabled by the Lewis acid sites on the RuO$_x$ phase. The calculated adsorption energies of furfural and FA on Ru(0001) surface are more than 1.2 eV higher than that of 2-propanol (Table 2), suggesting site-blocking by furfural and FA on metallic Ru sites is likely. In contrast, 2-propanol adsorbs more strongly on RuO$_2$(110) than on the metal, and given its excess, it could dominate on the oxide surface. This indicates that the metal-mediated dehydrogenation of 2-propanol and hydrogenation of furfural are heavily
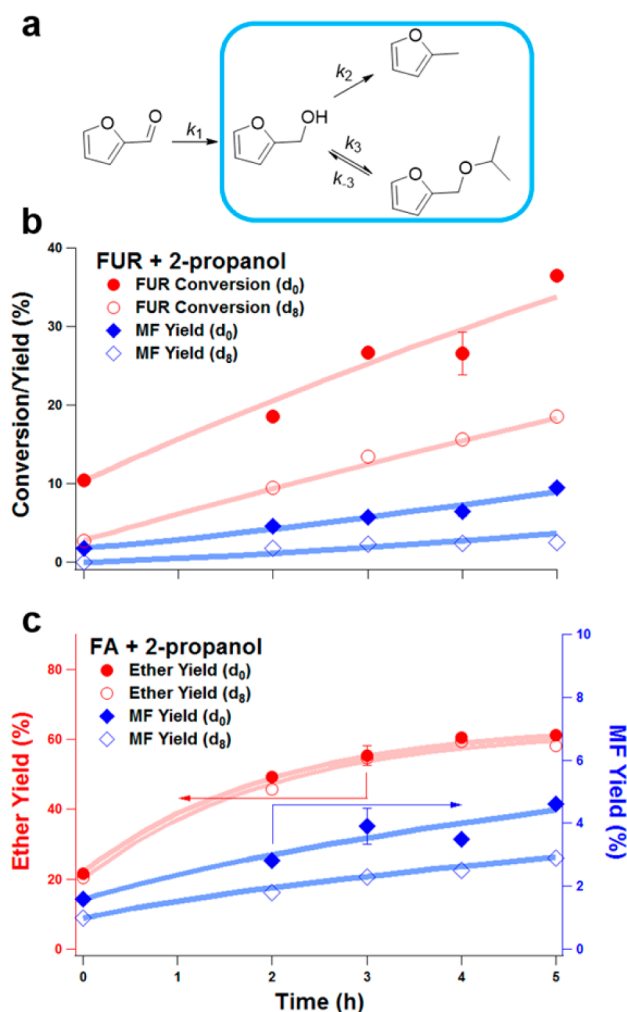

Figure 3. Kinetic studies of the HDO of furfural and FA. (a) Proposed reaction network. Product distribution as a function of time and fittings based on proposed kinetic model for hydrogenolysis of (b) furfural and (c) FA with 2-propanol-d_0 (solid symbols) or d_8 (open symbols). Experimental conditions: 1 wt % FA in 10% 2-propanol-d_0 or -d_8 in toluene solution, C_{cat} = 4.1 g L^{-1}, 2.04 MPa N$_2$.

suppressed by the high coverage of furfural and FA, whereas the MPV pathway is relatively facile because of the better accessibility of 2-propanol to Lewis acid sites. The inability of the intermolecular hydride transfer to facilitate the C−OH bond scission in FA necessitates metal-mediated (albeit slow) dehydrogenation of 2-propanol. Meanwhile, our previous work clearly showed that metallic Ru alone was inferior to the metal/Lewis acid combination in the formation of MF.[37,38] We hypothesize that the relatively accessible Lewis acid sites contribute to the hydrogenolysis of C−OH bond by receiving the OH (Figure 2a). The high adsorption energy of FA on RuO$_2$(110) indicates that high concentrations of FA will likely limit the access of 2-propanol to Lewis acid sites and lead to a lower rate of hydrogenolysis, which is consistent with the observation that k_2 is more than 1 order of magnitude smaller when FA is the reactant, as compared with when starting with furfural.

Although the design of bifunctional HDO catalysts remains a challenge, mechanistic insights gained in this work could guide the development of more selective catalysts for the reaction cascade of converting furfural to MF. One key aspect in the

Table 1. Estimated Equilibrium Rate Constants and KIE Values

rate/eq constant	Furfural +2-propanol			FA + 2-propanol		
	d_0 (L mol^{-1} h^{-1})	d_8 (L mol^{-1} h^{-1})	KIE	d_0 (L mol^{-1} h^{-1})	d_8 (L mol^{-1} h^{-1})	KIE
k_1	0.08	0.048	1.7			
k_2	0.28	0.23	1.3	0.016	0.010	1.6
k_3	1.1	1.1	1.0	0.43	0.42	1.0
K_3	4.3	4		2.8	2.4	

Table 2. Binding Energies on Ru(0001) and RuO$_2$(110) Obtained Using Density Functional Theory Calculations

molecule	Ru(0001), eV	RuO$_2$(110), eV
furfural	−1.54	−1.13
FA	−1.52	−1.76
2-propanol	−0.27	−1.35
ether	−1.34	−0.40

design of HDO catalysts is optimizing the oxophilicity of the metal component: less oxophilic metals than Ru could reduce the site-blocking by oxygenates and thus increase overall reaction rates; at the same time, it is clear that the oxophilic nature of Ru is a prerequisite for the existence of the RuO$_x$ phase, which provides Lewis acid sites, under the reducing environment of HDO reactions. Supporting metal on Lewis acidic supports (e.g., Al$_2$O$_3$, TiO$_2$ and Sn-Beta) could be a strategy to decouple the two functionalities and provide further insights. This hypothesis is supported by work by Dumesic et al., who showed facile MPV-hydrogenation of levulinate esters to γ-valerolactone over metal oxides under conditions similar to those of this work.[10] Another arguably more promising strategy is to employ bimetallic alloys and selectively oxidize the more oxophilic component to ensure atomic contact of metal and Lewis sites. Rh−ReO$_x$/SiO$_2$[38] is a good example in which the more oxophilic Re is selectively oxidized while Rh remains metallic. Furthermore, the fundamental insights discussed above are expected to be able to extend to other HDO/CTH reactions involving reactants with similar structures and functional groups, for example, furan ring hydrogenation and opening, and conversion of other biomass derivatives, for example, HMF to 2,5-dimethylfuran.

CONCLUSIONS

To summarize, a molecular level understanding of the mechanistic steps leading to the hydrodeoxygenation of furfural to MF on a bifunctional Ru/RuO$_x$/C catalyst via CTH has been mapped out via a combination of isotopic labeling experiments with detailed mass fragmentation analysis and kinetic studies. Hydrogenation of the carbonyl group in furfural to a hydroxymethyl group proceeds via the Lewis acid-catalyzed intermolecular hydride transfer (MPV) mechanism rather than dehydrogenation of the donor, followed by hydrogenation of the carbonyl group on metal sites. Given the facile dehydrogenation ability of the alcohol donor under the same conditions, we propose that strong adsorption of furfural retards the metal-catalyzed channel but does not affect the MPV channel because of the concerted nature of this path whereby IPA hydrogen bonds to the furfural (no need for site competition). Hydrogenolysis of the C−OH bond in FA to MF may occur via a direct path of dehydroxylation and hydrogenation on metal sites but mainly via ring activation whereby the ring gets hydrogenated at the C$_3$ position, leading to loss of aromaticity followed by C−OH bond scission on Lewis acid sites. In the

latter mechanism, the metal sites serve mainly to produce hydrogen from the donor and the Lewis acid RuO$_x$ sites to carry out hydrogenolysis. Furthermore, significant KIEs were observed in both the hydrogenation and hydrogenolysis steps. The former is consistent with the MPV mechanism as the dominant pathway; the latter suggests that a C−H bond scission, rather than C−O bond scission, is rate-limiting in the hydrogenolysis of FA. The molecular-level understanding gained regarding the reaction pathway lays the foundation for the development of efficient catalytic process for this and similar cascade reactions.

ASSOCIATED CONTENT

Ⓢ Supporting Information

The Supporting Information is available free of charge on the ACS Publications website at DOI: 10.1021/acscatal.5b00586.

Additional experimental details, calculations, figures, schemes, and references (PDF)

AUTHOR INFORMATION

Corresponding Authors
*E-mail: vlachos@udel.edu.
*E-mail: bxu@udel.edu.

Notes
The authors declare no competing financial interest.

REFERENCES

(1) Sutton, A. D.; Waldie, F. D.; Wu, R.; Schlaf, M.; Silks, L. A., III; Gordon, J. C. *Nat. Chem.* **2013**, *5*, 428−432.
(2) Yan, N.; Yuan, Y.; Dykeman, R.; Kou, Y.; Dyson, P. J. *Angew. Chem., Int. Ed.* **2010**, *49*, 5549−5553.
(3) Zhao, C.; Song, W.; Lercher, J. A. *ACS Catal.* **2012**, *2*, 2714−2723.
(4) Zhu, X.; Lobban, L. L.; Mallinson, R. G.; Resasco, D. E. *J. Catal.* **2011**, *281*, 21−29.
(5) Rahimi, A.; Ulbrich, A.; Coon, J. J.; Stahl, S. S. *Nature* **2014**, *515*, 249−252.
(6) Wang, G. H.; Hilgert, J.; Richter, F. H.; Wang, F.; Bongard, H. J.; Spliethoff, B.; Weidenthaler, C.; Schuth, F. *Nat. Mater.* **2014**, *13*, 293−300.
(7) Jae, J.; Zheng, W. Q.; Lobo, R. F.; Vlachos, D. G. *ChemSusChem* **2013**, *6*, 1158−1162.
(8) Scholz, D.; Aellig, C.; Hermans, I. *ChemSusChem* **2014**, *7*, 268−275.
(9) Tuteja, J.; Choudhary, H.; Nishimura, S.; Ebitani, K. *ChemSusChem* **2014**, *7*, 96−100.
(10) Chia, M.; Dumesic, J. A. *Chem. Commun.* **2011**, *47*, 12233−12235.

(11) Hansen, T. S.; Barta, K.; Anastas, P. T.; Ford, P. C.; Riisager, A. *Green Chem.* **2012**, *14*, 2457−2461.

(12) Gandarias, I.; Arias, P. L.; Fernández, S. G.; Requies, J.; El Doukkali, M.; Güemez, M. B. *Catal. Today* **2012**, *195*, 22−31.

(13) Nagaraja, B. M.; Padmasri, A. H.; Raju, B. D.; Rama Rao, K. S. *Int. J. Hydrogen Energy* **2011**, *36*, 3417−3425.

(14) Panagiotopoulou, P.; Vlachos, D. G. *Appl. Catal., A* **2014**, *480*, 17−24.

(15) Panagiotopoulou, P.; Martin, N.; Vlachos, D. G. *J. Mol. Catal. A: Chem.* **2014**, *392*, 223−228.

(16) Barbaro, P.; Liguori, F.; Linares, N.; Marrodan, C. M. *Eur. J. Inorg. Chem.* **2012**, *2012*, 3807−3823.

(17) Climent, M. J.; Corma, A.; Iborra, S. *Chem. Rev.* **2011**, *111*, 1072−1133.

(18) Van de Vyver, S.; Geboers, J.; Jacobs, P. A.; Sels, B. F. *ChemCatChem* **2011**, *3*, 82−94.

(19) Chang, C.-C.; Green, S. K.; Williams, C. L.; Dauenhauer, P. J.; Fan, W. *Green Chem.* **2014**, *16*, 585.

(20) Cheng, Y.-T.; Huber, G. W. *Green Chem.* **2012**, *14*, 3114.

(21) Williams, C. L.; Chang, C. C.; Do, P.; Nikbin, N.; Caratzoulas, S.; Vlachos, D. G.; Lobo, R. F.; Fan, W.; Dauenhauer, P. J. *ACS Catal.* **2012**, *2*, 935−939.

(22) Kresse, G.; Hafner, J. *Phys. Rev. B: Condens. Matter Mater. Phys.* **1993**, *47*, 558.

(23) Kresse, G.; Hafner, J. *Phys. Rev. B: Condens. Matter Mater. Phys.* **1994**, *49*, 14251.

(24) Kresse, G.; Furthmüller, J. *Comput. Mater. Sci.* **1996**, *6*, 15−50.

(25) Kresse, G.; Furthmüller, J. *Phys. Rev. B: Condens. Matter Mater. Phys.* **1996**, *54*, 11169.

(26) Blöchl, P. E. *Phys. Rev. B: Condens. Matter Mater. Phys.* **1994**, *50*, 17953.

(27) Kresse, G.; Joubert, D. *Phys. Rev. B: Condens. Matter Mater. Phys.* **1999**, *59*, 1758.

(28) Perdew, J. P.; Burke, K.; Ernzerhof, M. *Phys. Rev. Lett.* **1996**, *77*, 3865.

(29) Monkhorst, H. J.; Pack, J. D. *Phys. Rev. B* **1976**, *13*, 5188.

(30) Corma, A.; Domine, M. E.; Nemeth, L.; Valencia. *J. Am. Chem. Soc.* **2002**, *124*, 3194−3195.

(31) Corma, A.; Domine, M. E.; Valencia, S. *J. Catal.* **2003**, *215*, 294−304.

(32) Moliner, M.; Roman-Leshkov, Y.; Davis, M. E. *Proc. Natl. Acad. Sci. U. S. A.* **2010**, *107*, 6164−6168.

(33) Roman-Leshkov, Y.; Moliner, M.; Labinger, J. A.; Davis, M. E. *Angew. Chem., Int. Ed.* **2010**, *49*, 8954−8957.

(34) Stein, S. E. In *NIST Chemistry WebBook*; Linstrom, P. J., Mallard, W. G., Eds.; NIST standard reference database number 69; National Institute of Standards and Technology: Gaithersburg, MD, 2009; available at <http://webbook.nist.gov>.

(35) Bureiko, S. F.; Denisov, G. S. *Polym. J. Chem.* **2002**, *76*, 1177−1190.

(36) Bureiko, S. F.; Denisov, G. S. *J. Mol. Struct.* **2004**, *700*, 49−53.

(37) Jae, J.; Zheng, W.; Karim, A. M.; Guo, W.; Lobo, R. F.; Vlachos, D. G. *ChemCatChem* **2014**, *6*, 848−856.

(38) Chia, M.; Pagan-Torres, Y. J.; Hibbitts, D.; Tan, Q.; Pham, H. N.; Datye, A. K.; Neurock, M.; Davis, R. J.; Dumesic, J. A. *J. Am. Chem. Soc.* **2011**, *133*, 12675−12689.